IJST, Transactions of Civil Engineering, Vol. 35, No. C2, pp 199-215
Printed in The Islamic Republic of Iran, 2011

SHEAR WAVE VELOCITY-BASED LIQUEFACTION RESISTANCE OF SAND-SILT MIXTURES: DETERMINISTIC VERSUS PROBABILISTIC APPROACH*

R. DABIRI[1**] F. ASKARI, A. SHAFIEE & M. K. JAFARI[2]

[1]Dept. of Civil Engineering, Science and Research Branch, Islamic Azad University, Tehran, I. R. of Iran
Email: rouzbeh_dabiri@yahoo.com
[2]Geotechnical Engineering Research Center, International Institute of Earthquake Engineering and Seismology (IIEES), Tehran, I. R. of Iran

Abstract– Laboratory data that relates the liquefaction resistance of sand and silt mixtures to shear wave velocity are presented and compared to the liquefaction criteria derived from seismic field measurements based on the deterministic and probabilistic methods. In the deterministic method, cyclic triaxial and resonant column tests were conducted on specimens of Firoozkooh clean sand and sand-silt mixtures with a silt content up to 60% at different densities (*Dr* =15, 30, 60 and 75%). Cyclic undrained strength (*CRR*) and small strain shear wave velocity were determined for identical specimens formed using the undercompaction method and laboratory results were converted to field and compared to liquefaction criteria derived from seismic field measurements in previous research. In the probabilistic method, the three-sigma rule was used to analyze the uncertainty factors in liquefaction hazard analysis based on laboratory data. Probabilistic diagrams were also compared with that of other researchers. Results show that the use of the existing field-based correlations to assess *CRR* is overestimated in comparison to field cyclic resistance evaluated by laboratory testing for the Firoozkooh sand-silt mixtures containing 60% fines. For clean sand and specimens containing up to 30% fines, the results of this study on cyclic resistance were fairly consistent with previously published results.

Keywords– Non-plastic fines, liquefaction resistance, shear wave velocity, field performance data, sand skeleton, cyclic triaxial test, resonant column test, probabilistic analysis

1. INTRODUCTION

Predicting the liquefaction resistance of soils is an important aspect of geotechnical earthquake engineering practice. Several evaluating procedures have evolved over the past three decades since a simplified method was pioneered by Seed and Idriss [1]. Although penetration-based methods (*SPT*, *CPT*) are well developed [2, 3], penetration tests may be impractical or unreliable at some sites. Also, shear wave velocity (V_s) offers engineers a promising alternative and supplementary tool to evaluate liquefaction resistance of soils. The use of V_s as an index of liquefaction resistance has a sound basis because both V_s and liquefaction resistance are similarly, but not proportionally, influenced by many of the same factors (void ratio, state stress, stress history, geologic age).

The advantages of a V_s-based method have been discussed by many researchers [2,4]. Over the past few years, the V_s-based procedure for liquefaction assessment has attracted numerous studies and progressed significantly with improved correlations and more complete data bases [4]. The prevailing approach involves in-situ V_s measurements at sites experiencing earthquakes [5,6] following the framework of the Seed and Idriss [1] simplified procedure and correlating the overburdened stress-

*Received by the editors April 25, 2010; Accepted December 21, 2010.
**Corresponding author

corrected shear wave velocity (V_{s1}) to the magnitude-scaled cyclic stress ratio (*CSR*) induced by earthquakes. However, these in-situ V_s-based methods are still less well defined, mainly because of the lack of field performance data [7].

Most measured soil parameters for in-situ V_s testing are for post earthquake properties and do not exactly reflect the initial soil states before earthquakes. Thus, despite their great practical importance, field CRR-V_{s1} correlations do not furnish insight into the fundamental behavior of liquefiable soils. As pointed out by Seed and Idriss [1], if field seismic conditions are properly simulated, controlled laboratory studies can be used to broaden the applicability of liquefaction criteria, especially where little or no field performance data is available. A number of studies have focused on this subject on clean sands and sand-silt mixtures [8-17] that demonstrated the validity of laboratory V_s-based methods. Despite major uncertainties, the evaluation of liquefaction potential of soils is still routinely carried out by deterministic approaches. However, methods for probabilistic and statistical liquefaction risk analysis have been available for more than two decades.

In this study, deterministic and probabilistic methods were used and compared using V_s-based liquefaction potential assessment. First, in the deterministic approach, cyclic triaxial and resonant column tests were conducted on reconstituted specimens of clean sand and sand-silt mixtures prepared at different densities. In this way, liquefaction resistance and shear wave velocity were measured in identical laboratory specimens. The data obtained from this study, along with existing data, were transferred to the field and compared with field performance curves proposed by Andrus and Stokoe [4]. The experimental investigations focused on clean sand and sand containing up to 60% non-plastic silt. The high silt content samples were tested to overcome the shortage of the laboratory data in this region.

Next, a probabilistic approach based on CRR_{field}-V_{s1} laboratory data using the three-sigma rule was performed and probability diagrams were compared with the probabilistic curves in Kayen et al. [18]. This study seeks to clarify the differences between the conventional deterministic and probabilistic methods using the V_s-based liquefaction evaluation of Firoozkooh Sand-Silt mixtures.

2. TESTING MATERIAL AND PROCEDURE

a) Tested soils

Firoozkooh sand (#161), uniformly graded sand (*SP*) with a mean grain size of 0.25 mm, was used. Its grains are sub-angular to sub-round in shape. The non-plastic silt used in the testing program was derived from the fine-grained portion of Firoozkooh silty sand. Figure 1 shows the grain size distributions of the soils used.

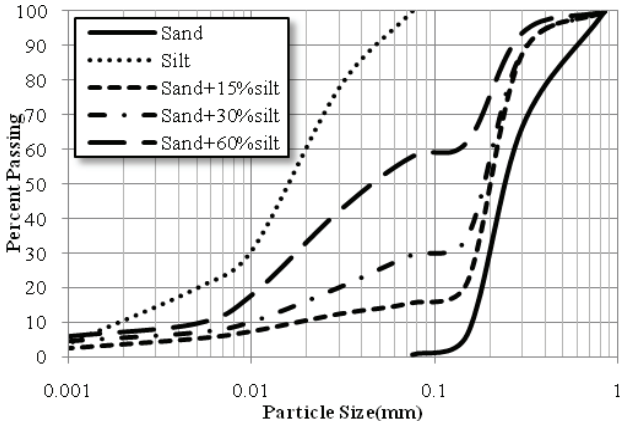

Fig. 1. Grain size distribution for soils used in this study

Clean sand with three mixtures of sand-silt was used. The mixtures were obtained by mixing 15, 30, and 60% of silt, respectively, with sand. The specimens were prepared to achieve after-consolidation relative densities of 15, 30, 60 and 75% depending on their silt content. The global void ratios (e) and the sand skeleton void ratios (e_s) for the mixtures are presented in Table 1. The sand skeleton void ratio exists in a silty sand when all of the silt particles are removed, leaving only the sand grains and voids to form the skeleton. The vibratory table method (ASTM D4253) was used to determine minimum void ratio, e_{min}. ASTTM D4254 was employed to find the maximum void ratio, e_{max}.

Table1. Values of e and e_s for different mixtures

Type of materials	e_{min}	e_{max}	*Dr=15%*		*Dr=30%*		*Dr=60%*		*Dr=75%*	
			e	e_s	e	e_s	e	e_s	e	e_s
Sand	0.58	0.87	0.83	0.83	0.78	0.78	0.69	0.69	0.65	0.65
Sand+15%Silt	0.41	0.83	0.76	1.08	0.7	1	0.58	0.86	0.51	0.57
Sand+30%Silt	0.32	0.854	0.77	1.52	0.69	1.41	0.53	1.185	0.45	1.07
Sand+60%Silt	0.36	1.259	1.124	-	0.99	-	0.72	-	0.58	-

b) Method of sample preparation

In order to obtain a uniform density throughout the specimen, the undercompaction technique of Ladd [19] was used. This consists of placing each layer at a density slightly greater than the density of the layer below it to account for the decrease in volume and increase in density that occurs in the lower layers when a new layer is placed on it. The specimens were made in six layers with an undercompaction value of 5%, so that relative density varied by 1% per layer. To ensure uniform density throughout the specimen height, the void ratio distribution within the specimen was obtained by solidifying a specimen using a gelatin solution [20]. The solidified specimen was then sliced into sections and the distribution of void ratio within the test specimen was determined. The measurements revealed that the relative error in achieving the required density throughout the specimens was successfully less than 5% for each layer. In addition, the specimens were prepared in a Plexiglas mold to have better control over layer thickness. During sample preparation, it was found that forming low density specimens for high silt content (i.e., 60%) materials was impossible because of excessive collapse during saturation. Thus, high silt content specimens were prepared at high relative densities of 60 and 75%, meanwhile other specimens were prepared at densities of 15, 30 and 60%.

c) Test procedure and results

The *CRR* values were measured using an automated stress-controlled cyclic triaxial by The Seiken-DTC 384-EP apparatus. The specimens were tested at a typical diameter of 70 mm and a height of 150 mm. Small strain shear wave velocity, V_s, was also measured using a fixed-free type, torsional resonant column by The Seiken DTC 384-EP apparatus (Characteristic of apparatus is shown in Table 2). The tested specimens were typically 70 mm in diameter and 100 mm in height. They were saturated with a Skempton B value in excess of 98%. To facilitate the saturation process, carbon dioxide (CO_2) was percolated through the specimens and then de-aired water was flushed into the specimens. Finally, a back pressure of 100 kPa was incrementally applied to accelerate the saturation rate and the specimens were isotropically consolidated under an effective confining stress of 100 kPa. All relative densities reported herein were based on the after-consolidation void ratios.

Table 2. Characteristics of cyclic triaxial and resonant column apparatus

Characteristic of cyclic triaxial apparatus	
Capacity of lifter jack	50(kN)
Capacity of vertical load	2(kN)
Maximum of confining and back pressure	±1000(kPa)
Frequency of loading	0.001-100 Hz
Maximum of specimen diameter	7 (Cm)
Maximum of specimen height	14(Cm)
Characteristic of resonant column apparatus	
Shear strain amplitude (%)	10^{-2}-10^{-4}
Maximum of confining pressure	±1000(kPa)
Maximum of specimen diameter	7(Cm)
Maximum of specimen height	14(Cm)

In the cyclic triaxial tests, the specimens were loaded sinusoidally at a frequency of 0.1 Hz ASTM D5311 varying deviator stress at the appropriate cyclic stress ratio until they liquefied. Resonant frequencies and amplitude of vibration measured in the resonant column tests, along with a system calibration, were also used to determine V_s. In the present study, liquefaction was defined and evaluated at initial liquefaction when the pore pressure in the specimen first equaled the initial confining stress or the specimen reached a 5% double amplitude axial strain, whichever occurred first. Cyclic resistance was defined as the cyclic stress ratio required to cause initial liquefaction in 15 cycles of loading [21]. The results of the cyclic triaxial and resonant column tests are presented in Fig. 2 and Table 3.

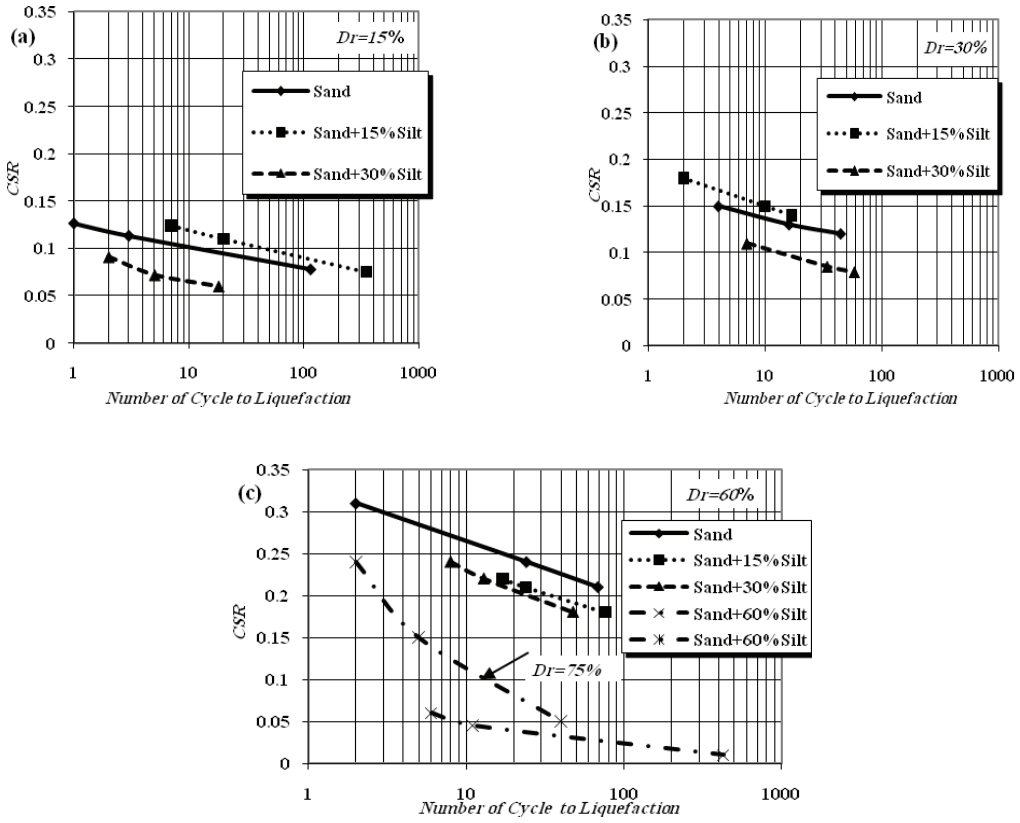

Fig. 2. Results of cyclic triaxial tests for the various combinations of sand with silt
(a) *Dr*=15% (b) *Dr* =30% and (c) *Dr* =60 and75%

Table 3. Results of cyclic triaxial and resonant column tests of sand and silt mixtures

Type of material	*Dr*	$CRR_{Triaxial}$	*Vs(m/s)*	G_{max} *(kPa)*	*D (%)*
Sand	0.15	0.096	182	52500	4.7
	0.30	0.132	193	74200	4.5
	0.60	0.25	201	85500	4.3
Sand+15%Silt	0.15	0.112	169	45200	4
	0.30	0.142	181	57500	3.8
	0.60	0.23	202	74400	3.5
Sand+30%Silt	0.15	0.061	157	32500	3.8
	0.30	0.096	168	44600	3.6
	0.60	0.23	189	69100	3.4
Sand+60%Silt	0.60	0.033	164	45900	3.6
	0.75	0.093	175	57300	3.7

As shown in Figs. 2a, b and c and Tables1 and 3:

- In very loose and medium dense materials (*Dr* = 15 and 30%), the cyclic resistance of Firoozkooh sand first slightly increased with fines content up to 15%, then decreased beyond this value. A similar trend was found by Koester [22] in testing on the mixtures of fine sand and non-plastic silt.
- In dense samples (*Dr* = 60%), the cyclic resistance of Firoozkooh sand continuously decreased with silt content. The cyclic resistance of the specimens containing 60% silt with *Dr* = 75% are shown on Fig. 2(c). As expected, cyclic resistance increased with relative density.
- The cyclic resistance ratio increased with the sand skeleton void ratio for mixtures having up to 15% silt and decreased with further increases of the silt content. In dense specimens (*Dr* = 60%), *CRR* continually decreased with the sand skeleton void ratio.
- Shear wave velocity, V_s, continuously decreased with the sand skeleton void ratio and silt content, and increased with relative density.
- The maximum shear modulus (G_{max}) increased with relative density. On the other hand, G_{max} decreased as the fines content increased up to 30%. It then increased with a fines content of more than 30%.
- The damping ratio (*D*) decreased when relative densities increased and fines content increased up to 30%. Then it increased slightly with fines content up to 60%.

To date, no clear consensus has been reached on the influence of non-plastic fines on the cyclic resistance of sands. Some researchers concluded that fines increase the liquefaction resistance [23-27]. Others indicated that fines decrease the liquefaction resistance [28-31]. Still other studies have found that sand resistance to liquefaction initially decreases as the silt content increases until a minimum resistance is reached and then increases as the silt content increases [32-36].

The effect of fines on the shear wave velocity has been studied less completely and not well-understood. Resonant column tests conducted by Iwasaki and Tatsuoka [37] and bender element tests performed by Salgado et al. [36] and Huang et al. [12] showed that the small strain-shear modulus, G_{max}, and, therefore, V_s decreased with an increase in non-plastic fines content. These seemingly contradictory conclusions may stem from factors including: (1) using different deposition methods for specimen preparation; (2) testing sands with different silt contents and densities; (3) testing specimens under different confining stresses and loading conditions; and (4) using different criteria to define liquefaction and cyclic shear resistance.

d) Conversion of laboratory data to field condition

Both the *CRR* and V_s were obtained in the undrained cyclic triaxial and resonant column tests under isotropic consolidation conditions, which are usually different from the in-situ conditions required to be

evaluated for design purpose. Therefore, some consideration should be given to applying the laboratory test-based *CRR*-V_s correlation to in situ conditions. It is common to correct *CRR* to in situ *CRR* (CRR_{field}) approximately as follows [38]:

$$CRR_{field} = \alpha.\beta.CRR_{triaxial} \tag{1}$$

where α and β are correction factors. Constant α can be presented by a number of equations, such as:

$$\alpha = K_0 \tag{2}$$

$$\alpha = \frac{1+2K_0}{3} \tag{3}$$

$$\alpha = \frac{1+K_0}{2} \tag{4}$$

$$\alpha = \frac{2(1+2K_0)}{3\sqrt{3}} \tag{5}$$

in which K_0 is the effective earth pressure ratio at rest. Eqs. (2) and (3) were proposed by Seed and Peacock [38], Eq. (4) by Finn et al. [39] and Eq. (5) by Castro [40]. Coefficient K_0 was also considered as equal to $(1-\sin\varphi')$, where φ' is the angle of internal friction. For each mixture at a specific relative density, φ' was determined using monotonic undrained triaxial tests conducted under initial confining stresses of 100, 200 and 300 kPa (Table 4). Finally, by averaging over the α values from Eqs. (2) to (5), the desired value of constant α was determined (α_{mean} in Table 4).

Constant β is a function of relative density [41] and is defined as:

$$\begin{aligned} Dr \le 45\% &\Rightarrow \beta = 1.15 \\ Dr \succ 45\% &\Rightarrow \beta = 0.01Dr + 0.7 \end{aligned} \tag{6}$$

Table 4 presents the value of β along with CRR_{field} for different mixtures. On the other hand, the measured V_s required adjustment allowing for the different stress states. Since V_s was widely observed to depend equally upon principal stresses in the direction of wave propagation and particle motion [41], it can be expressed as:

$$V_{sf} = V_s\left[\frac{(1+2K_0)}{3}\right]^{0.25} \tag{7}$$

Where V_{sf} is the equivalent field value of laboratory measured V_s. According to common practice [4, 5], the V_{sf} in Eq. (7) should be further corrected in terms of the in-situ effective overburden stress (σ'_V) as follows[42]:

$$V_{s1} = V_{sf}\left(\frac{P_a}{\sigma'_V}\right)^{0.25} = V_s\left(\frac{1+2K_0}{3}\right)^{0.25}\left(\frac{P_a}{\sigma'_m}\right)^{0.25} \tag{8}$$

where V_{s1} is the overburden stress-corrected velocity; P_a is the atmosphere pressure and σ'_m is the mean effective stress in the laboratory. Table 4 presents the value of V_{s1} for each mixture.

Table 4. CRR_{field} and V_{s1} for different sand-silt mixtures

Type of material	*Dr*	$\varphi'(^\circ)$	$CRR_{triaxial}$	V_S (m/s)	α_{mean}	β	CRR_{field}	V_{S1} (m/s)
sand	0.15	20	0.096	182	0.788	1.15	0.087	170.6
	0.30	29	0.132	193	0.68	1.15	0.103	174.8
	0.60	34	0.25	201	0.63	1.3	0.201	178
Sand+15%Silt	0.15	17	0.112	169	0.83	1.15	0.106	160
	0.30	23	0.142	181	0.752	1.15	0.123	167
	0.60	32	0.23	202	0.65	1.3	0.194	181
Sand+30%Silt	0.15	16.2	0.061	157	0.832	1.15	0.058	149
	0.30	19	0.096	168	0.796	1.15	0.088	157
	0.60	29	0.23	189	0.68	1.3	0.203	171
Sand+60%Silt	0.60	28	0.033	164	0.69	1.3	0.03	149
	0.75	31	0.093	175	0.66	1.45	0.088	157

In Table 4, the values of CRR_{Field} increased as the silt content increased up to 15%. With a further increase in silt content up to 30%, cyclic resistance ratio decreased in lower relative densities (*Dr* = 15%, 30%). As the silt content increased up to 60%, the CRR_{Field} decreased in dense relative density (*Dr* = 60%). With an increase of relative density from 60% to 75%, the CRR_{Field} increased.

e) Comparison of converted laboratory results with field-based correlations

The CRR_{field}-V_{s1} correlations developed in the laboratory for this and other studies were compared to the field-based correlations of Andrus and Stokoe [4] for different ranges of fines content (*FC*) as:

1. Laboratory-based correlations for clean sands (*FC* = 5%) based on the data from this study, Tokimatsu et al. [43], Rouch et al. [11], Huang et al. [12], and Ning Liu et al.[15] (Fig. 3).
2. Laboratory-based correlations for silty sands with $5\% \prec FC \prec 30\%$ based on the data from this study, Rouch et al. [11], Huang et al. [12], and Ning Liu et al.[15] (Fig. 4).
3. Laboratory-based correlations for sand-silt mixtures (*FC* = 35%) based on the data from this study, Huang et al. [12] and Baxter et al. [17] (Fig. 5).

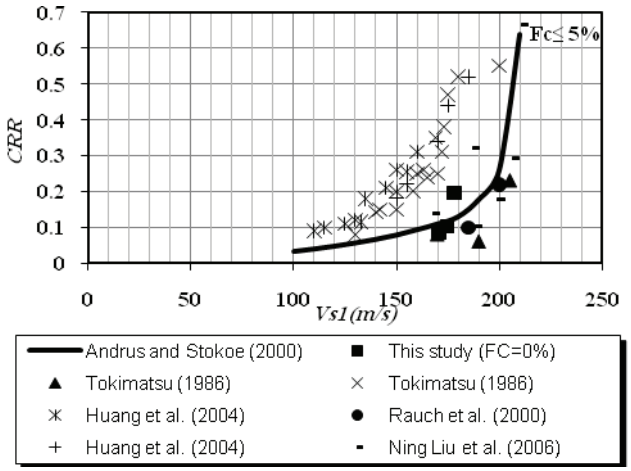

Fig. 3. Comparison between converted CRR_{field}-V_{s1} data based on the laboratory data from clean sand ($FC \le 5\%$) and the existing field-based correlation of Andrus and Stokoe [1]

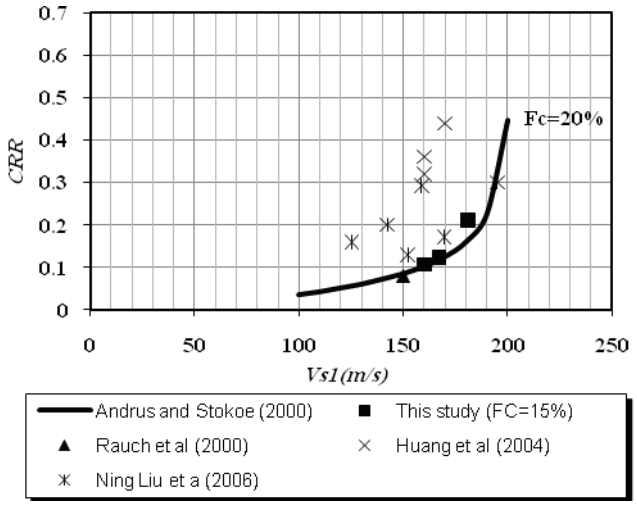

Fig. 4. Comparison between converted CRR_{field}-V_{s1} data based on the laboratory data from silty sands ($5\% \prec FC \prec 30\%$) and the existing field-based correlation of Andrus and Stokoe [1]

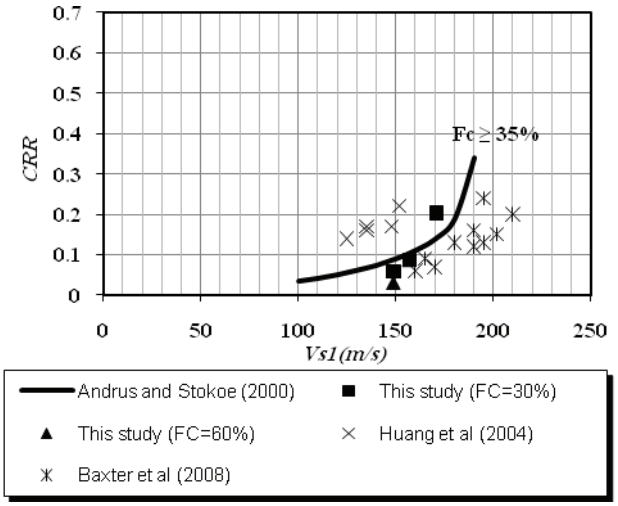

Fig. 5. Comparison between converted CRR_{field}-V_{s1} data based on the laboratory data from sand-silt mixtures ($FC \geq 30\%$) and the existing field-based correlation of Andrus and Stokoe [1]

Figure 3 shows that the CRR_{field}-V_{s1} correlation for the clean sand used in this study lies to the right of, but near, the semi-empirical curve proposed in the simplified procedure for fines content of less than 5%. Similarly, the trends in the laboratory data on sands with 15% fines content was found to be consistent with the liquefaction boundary curves developed by Andrus and Stokoe [4] for FC = 20% from the field performance data (Fig. 4).

As shown in Fig. 5, the laboratory-based correlations from this study for FC = 30 and 60% plot well below the field-based curve for $FC \geq 30\%$. Using the field-based correlations would overestimate the liquefaction resistance of these sand-silt mixtures. As seen in Fig. 5, significant differences may exist between laboratory-based correlations and the field performance data of Andrus and Stokoe [4]. This difference may originate from the inherent uncertainties in laboratory and field performance data. The uncertainties in laboratory data include:

1. Techniques used to form test specimens in the laboratory significantly affect the measured cyclic resistance and shear wave velocity.

2. The cyclic stress path generated by uniform cycles of axial stress in a triaxial test only approximately models an earthquake loading on a soil deposit.

3. The uncertainties of the relationship between laboratory and field conditions are only approximately accounted for in the correction of cyclic triaxial strength ($CRR_{triaxial}$) to in situ cyclic resistance ratios (CRR_{field}).

4. The measurement of cyclic strength and shear wave velocity in separate soil specimens also introduced a potential source of error.

The uncertainties in field performance data may also originate from:

1. The uncertainties in the plasticity of the fines in the in situ soils.
2. Using post earthquake properties that do not exactly reflect the initial soil states before earthquakes.
3. The assumption that the CRR_{field} is equal to the *CSR* obtained from Seed and Idriss [1]. This may result in a significant overestimation of CRR_{field} when the factor of safety is less than 1.

3. PROBABILITY ANALYSIS

An essential component of the art of geotechnical engineering is the ability to estimate reasonable values for parameters based on meager data or correlations from the results of in situ and index tests. As an alternative or supplement to the deterministic assessment [44], a probabilistic evaluation of liquefaction potential was assessed in terms of the probability of liquefaction. Often, the results of such probabilistic assessments lead to better engineering decisions.

A number of researchers have contributed to the subject of the statistical/probabilistic evaluation of liquefaction. Some have applied probability and statistics to the uncertainties associated with the simplified methods (Yegian and Withman [45]; Haldar and Tang [46]). Others have conducted logistic regression analyses of field performance data to establish empirical equations for interpreting the probability of liquefaction (Liao et al. [47]; Youd and Noble [48]; Toprak et al. [49]; Juang et al. [50], Andrus et al. [51]; Juang et al. [52]). The latter approach, first proposed by Liao et al. [47] has gained significant attention as a tool to characterize the liquefaction boundary curve (the curve that separates liquefaction from no liquefaction) in simplified methods.

Departing from the logistic regression approach, Cetin et al. [53]; Juang et al. [54] and Kayen et al. [18] used reliability analysis and Bayes' theorem to derive the probability of liquefaction. With their approach, a Bayesian mapping function that relates the reliability index and factor of safety was developed based on field performance data.

A general review of the research shows that results are mainly based on field performance data. To estimate P_f (the probability of factor of safety being less than 1), it is necessary to estimate the standard deviation of the parameters in the computation of the factor of safety. This can be carried out using the same types of judgments and evaluations used to estimate average parameter values. Depending upon the amount of available data, four methods, computation from data, published values, the three sigma rule and graphical three sigma rules, can be used to estimate the standard deviation of geotechnical parameters [55]. In this study, the graphical three sigma rules were used for probabilistic analysis.

a) Graphical three-sigma rule

The three sigma rule (3σ), described by Dai and Wang [56], uses the fact that 99.73% of all values of a normally distributed parameter fall within three standard deviations of the average [55]. Thus, if *HCV* equals the highest conceivable value of a parameter and *LCV* equals the lowest, approximately three standard deviations exist above and below the average value. The 3σ rule can be used to estimate the

standard deviation by first estimating the highest and lowest conceivable values of the parameter and then dividing the difference by 6:

$$\sigma = \frac{HCV - LCV}{6} \tag{9}$$

With the 3σ rule, it is possible to estimate standard deviation values using the same amounts and types of data that are used for conventional geotechnical analyses. The 3σ rule can be applied when only limited data are available. It uses simple normal distribution as a basis for estimating that the range of ±3 standard deviations covers virtually the entire population. For this analysis, test results from five types of sand (Toyoura, Niigata, Mai Liao, Monterey, Firoozkooh) were used. The data base for probabilistic analyses is shown in Table 5 and included the test results on:

- clean sands ($FC \leq 5\%$) from this study, Tokimatsu et al.[43], Rouch et al. [11], Huang et al. [12] and Ning liu et al.[15]
- silty sands with $5\% \prec FC \prec 30\%$ from this study, Rouch et al. [11], Huang et al. [12] and Ning Liu et al.[15]
- sand-silt mixtures ($FC \geq 30\%$) from this study, Huang et al. [12] and Baxter et al. [17]

b) The results of probabilistic analysis

The concept behind the 3σ rule can be extended to graphical procedures applicable to many aspects of geotechnical engineering. This rule was applied as follows:

1. A straight line or curve was drawn through the data representing the most likely average variation of the parameters by depth. In this study, the average curve definition (*PL=50%*) was drawn in a similar shape to Andrus and Stokoe [4] for $FC \leq 5\%$, $5\% \prec FC \prec 30\%$ and $FC \geq 30\%$. This resulted in the following equations based on the catalogue (Table 4):

$$FC \leq 5\% \Rightarrow CRR = 0.0576(\frac{V_{s1}}{100})^2 + \frac{1.101}{215 - V_{s1}} \tag{10}$$

$$5\% \prec FC \leq 30\% \Rightarrow CRR = 0.033(\frac{V_{s1}}{100})^2 + \frac{2.53}{209 - V_{s1}} \tag{11}$$

$$FC \succ 30\% \Rightarrow CRR = 0.0139(\frac{V_{s1}}{100})^2 + \frac{0.713}{200 - V_{s1}} \tag{12}$$

2. Straight lines or curves were drawn representing the highest and lowest conceivable bounds on the data (*PL*=1% and 99%). These should be wide enough to include all valid data and allow for the natural tendency to estimate such bounds too narrowly. It should be noted that some points are outside the estimated bounds, indicating that these data points may be erroneous.
3. Straight lines or curves representing the average plus one standard deviation and the average minus one standard deviation were drawn. These were one-third of the distance from the average line to the highest and lowest conceivable bounds (*PL*=32% and 68%).

These curves are shown in Figs. 6, 7 and 8, where they are compared with Andrus and Stokoe [4] field-performance diagrams. The results show that the probability curve corresponding to *PL*=32% agrees fairly well with the Andrus and Stokoe [4] field-performance curves for $FC \leq 5\%$ and $FC = 20\%$. When the silt content is raised (Fig. 8), the probability curves fall beneath the Andrus-

Stokoe [4] deterministic curve for $FC \geq 35\%$. In other words, the Andrus-Stokoe field-performance curve nearly coincides with the $PL = 99\%$ curve of the present study. It can be inferred that the field-performance curve for high fines content sands is non-conservative.

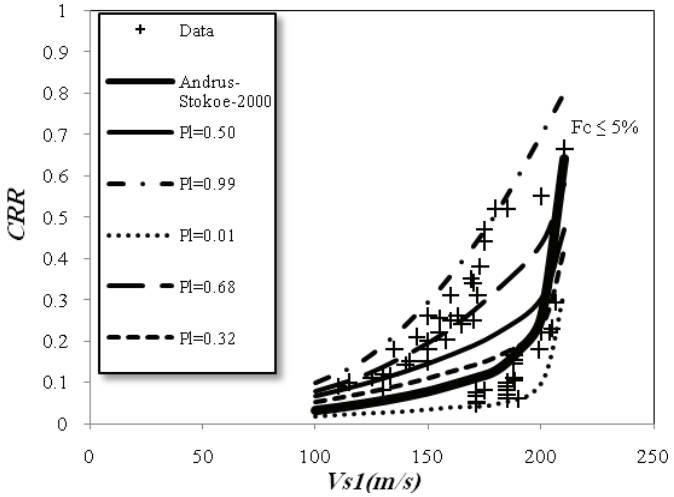

Fig. 6. Comparison of probability curves with deterministic Andrus and Stokoe [1] field-performance curve ($FC \leq 5\%$)

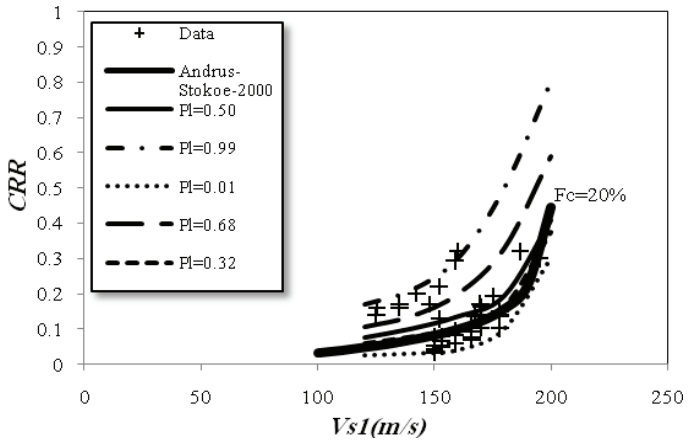

Fig. 7. Comparison of probability curves with deterministic Andrus and Stokoe [1] field-performance curve ($5\% \prec FC \leq 30\%$)

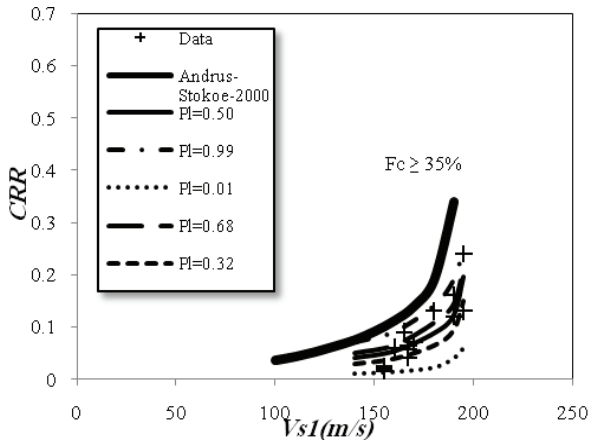

Fig. 8. Comparison of probability curves with deterministic Andrus and Stokoe [1] field-performance curve ($FC \succ 30\%$)

Table 5. Data base for probabilistic analysis

FC≤5%						5%<FC≤30%						FC>30%					
CRR	Vs1	FC	CRR	Vs1	FC	CRR	Vs1	FC	CRR	Vs1	FC	CRR	Vs1	FC	CRR	Vs1	FC
0.08	175	0	0.38	173	0	0.18	150	0	0.08	150	13	0.3	195	10	0.21	181	30	0.02	149	60	0.09	165	100
0.06	175	0	0.38	173	0	0.18	150	0	0.32	160	15	0.16	125	15	0.22	181	30	0.03	149	60	0.13	180	100
0.23	175	0	0.38	173	0	0.18	150	0	0.36	160	15	0.2	142	15	0.05	149	30	0.03	149	60	0.16	190	100
0.08	175	0	0.38	173	0	0.18	150	0	0.44	170	15	0.29	159	15	0.06	149	30	0.03	149	60	0.24	195	100
0.14	175	0	0.38	173	0	0.18	150	0	0.14	125	30	0.09	160	15	0.06	149	30	0.06	157	60			
0.15	175	0	0.38	173	0	0.18	150	0	0.16	135	30	0.1	160	15	0.06	149	30	0.08	157	60			
0.15	175	0	0.38	173	0	0.18	150	0	0.17	135	30	0.11	160	15	0.07	157	30	0.09	157	60			
0.20	175	0	0.38	173	0	0.18	150	0	0.17	148	30	0.11	160	15	0.09	157	30	0.1	157	60			
0.25	175	0	0.38	173	0	0.18	150	0	0.22	152	30	0.09	167	15	0.09	157	30	0.06	160	60			
0.26	175	0	0.38	173	0	0.18	150	0	0.14	168	15	0.12	167	15	0.1	157	30	0.07	170	100			
0.24	175	0	0.38	173	0	0.18	150	0	0.19	175	15	0.13	167	15	0.15	171	30	0.12	190	100			
0.25	175	0	0.38	173	0	0.18	150	0	0.32	187	15	0.14	167	15	0.2	171	30	0.13	195	100			
0.31	175	0	0.38	173	0	0.18	150	0	0.3	152	10	0.14	181	15				0.15	202	100			
0.35	175	0	0.38	173	0	0.18	150	0	0.17	170	10	0.2	181	15				0.2	210	100			
0.1	171	0	0.26	150	0	0.07	175	0															
0.13	178	0	0.23	178	0	0.1	175	0															
0.2	150	0	0.23	178	0	0.11	175	0															
0.21	145	0	0.2	150	0	0.12	178	0															

The probability curves of this study can be further verified by the recently reported in-situ *Vs* data. The first is the global *Vs* data base presented by Kayen et al. [18]. Figs. 9, 10 and 11 show probability curves proposed by Kayen et al. together with the present probabilistic *CRR*-V_{s1} curves and that of Andrus and Stokoe [4]. It can be seen that the probability curves for this study for $FC \leq 5\%$ and $FC = 20\%$ agree well with the proposed curves of Kayen et al. [18]. However, for $FC \geq 35\%$, the Kayen et al. probability curve of *PL*=5% is consistent with the probability curve of *PL*=68%.

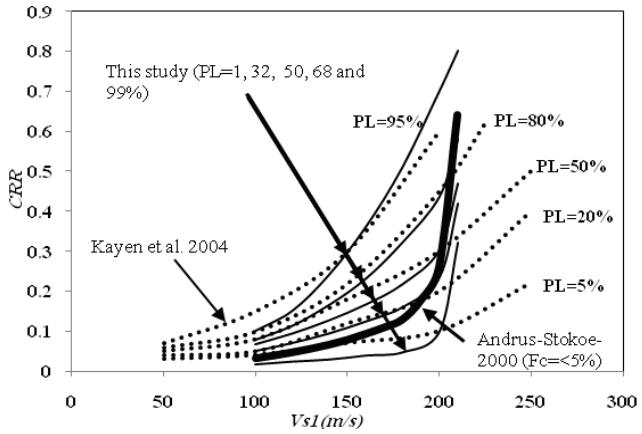

Fig. 9. Comparison of probability curves ($FC \leq 5\%$) with deterministic Andrus and Stokoe [1] field-performance curve and Kayen et. al. [18] probability curves

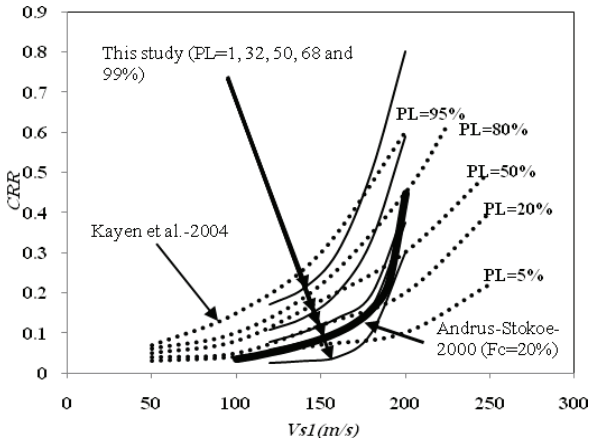

Fig. 10. Comparison of probability ($5\% \prec FC \leq 30\%$) curves with deterministic Andrus and Stokoe[1] field-performance curve and Kayen et. al. [18] probability curves

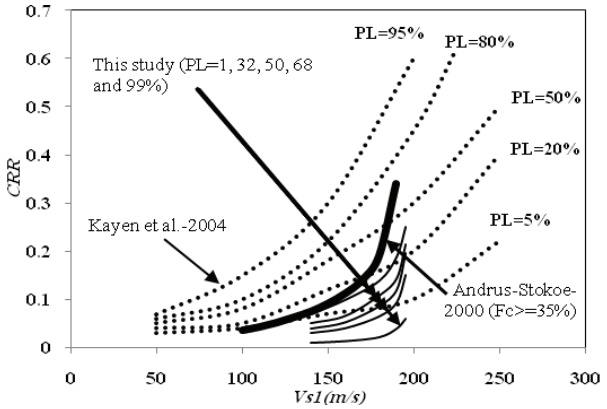

Fig. 11. Comparison of probability curves ($FC \succ 30\%$) with deterministic Andrus and Stokoe[1] field-performance curve and Kayen et. al. [18] probability curves

4. CONCLUSION

In this paper, the results of a new correlation between the cyclic resistance ratio and shear wave velocity (V_s) was developed for mixtures of Firoozkooh sand and non-plastic silt where the silt content varied from 0 to 60%. The specimens, prepared at different relative densities (from 15 to 75%), were tested in cyclic triaxial and resonant column apparatuses at 100 kPa initial effective confining stresses. Data from previous laboratory studies on sands, silty sands and the laboratory data generated as the part of this study were compared to field based CRR-V_{s1} curves prepared by Andrus and Stokoe [4]. Finally, a new probabilistic method for evaluating liquefaction potential of soils by using the 3σ rule for laboratory data was investigated and compared with Kayen et al. [4] probabilistic curves. Based on the shear wave velocity of sands, the following conclusions regarding the effects of non-plastic fines on the liquefaction susceptibility can be drawn:

- In very loose and medium dense materials (Dr = 15 and 30%), the CRR of Firoozkooh sand increased slightly with a fines content of up to 15%, followed by a decrease beyond this value. In dense samples (Dr = 60%), the cyclic resistance ratio of Firoozkooh sand continuously decreased with silt content. The cyclic resistance of the specimens containing 60% silt with Dr = 75%, cyclic resistance increased with relative density.
- In general, when the fines content is raised, the stability of the mixture fabric is reduced. Data obtained on the cyclic resistance, shear wave velocity and dynamic properties of the mixtures evidently show that, CRR, V_s, G_{max} and damping ratio have good correlations with skeleton void ratios. It can be concluded that an increase in fines content leads to a decrease in cyclic strength, shear wave velocity, maximum shear modulus and damping ratios.
- In the conversion of laboratory data to field conditions, the CRR_{field}-V_{s1} correlation for clean sand lies closely to the semi-empirical curve proposed in the simplified procedure for fines content of less than 5% by Andrus and Stokoe [4]. This trend was also observed in the converted laboratory data of this study on sands with 15% fines content. The results are also consistent with the liquefaction boundary curves developed by Andrus and Stokoe [4] for FC = 20%. The CRR_{field}-V_{s1} values for FC = 30 and 60% in the present research were below the field-based curve for $FC \geq$ 35%, meaning that field-based correlations overestimate the liquefaction resistance of these sand-silt mixtures in the present study.
- As an alternative or supplement to the deterministic assessment, a probabilistic evaluation of liquefaction potential was assessed. Probability calculations provide a means of evaluating the combined effects of uncertainties and of distinguishing between conditions where uncertainties are particularly high or low. The results show that the probability curve corresponding to PL = 32% agrees fairly well with the Andrus and Stokoe [4] field performance curves for $FC \leq$ 5% and $FC \leq$ 20%. When the silt content increased, the probability curves fell beneath the Andrus and Stokoe deterministic curve for FC = 35%. In other words, the Andrus-Stokoe field performance curve nearly coincided with the PL = 99% curve of the present study. It can be inferred that the field-performance curve for high fines content sands is non-conservative.

The probability curves for this study for $FC \leq$ 5% and FC = 20% agree well with Kayen et al. [18] curves for FC = 35%. However, for FC = 35%, the PL = 5% curve was consistent with the probability curve of PL = 68%. Note that specimen preparation, dimensions, fabric structure (different relative densities), and non-plastic fines content can influence the final results. These findings suggest the need for further evaluation of the effects of these parameters on probabilistic diagrams.

Acknowledgements: This research was conducted in and supported by the International Institute of Earthquake Engineering and Seismology (*IIEES*) under the Contract No.6712. This support is gratefully appreciated.

REFERENCES

1. Seed, H. B. & Idriss I. M. (1971). Simplified procedure for evaluating soil liquefaction potential. *Journal of Soil Mechanics and Foundation Division*, Vol. 97, No. 9, pp. 1249-1273.
2. Youd, T. L., Idriss, I. M., Andrus, R. D., Arango, R. C., Castro, G., Christian, J. T., Dobry, R., Finn, W. D. L., Harder, Jr., L. F., Hynes, M. E., Ishihara, K., Koester, J. P., Liao, S. S. C., Marcuson, III, W. F., Martin, G. R., Mitchell, J. K., Moriwaki, Y., Power, M. S., Robertson, P. K., Seed, R. B. & Stokoe, II, K. H. (2001), Liquefaction resistance of soils: Summary report from the 1996 NCEER and 1998 NCEER/NSF workshop on evaluation of liquefaction resistance of soils. *Journal of Geotechnical and Geoenvironmental Engineering*, Vol. 127, No. 10, pp. 817-833.
3. Idriss, I. M. & Boulanger, R. W. (2006), Semiempirical procedures for evaluating liquefaction potential during earthquakes. *Journal of Soil Dynamic and Earthquake Engineering*, Vol. 26, No. 2-4, pp. 115-130.
4. Andrus, R. D. & Stokoe, II. K. H. (2000). Liquefaction resistance of soils from shear wave velocity. *Journal of Geotechnical and Geoenvironmental Engineering*, Vol. 126, No. 11, pp. 1015-1025.
5. Robertson, P. K., Woeller, D. J. & Finn, W. D. L. (1992). Seismic cone penetration Test for evaluating liquefaction potential under cyclic loading. *Canadian Geotechnical Journal*, Vol. 29, No. 4, pp. 686-695.
6. Andrus, R. D., Stokoe, II. K. H. & Juang, C. H. (2004). Guide for shear wave-based liquefaction potential evaluation. *Earthquake Spectra*, Vol. 20, No. 2, pp. 285-308.
7. Kayen, R., Seed, R. B., Moss, R. E., Cetin, K. O., Tanaka, Y. & Tokimatsu, K. (2004). Global shear wave velocity database for probabilistic assessment of the initiation of seismic-soil liquefaction. *11th Int. Conference on Soil Dynamics and Earthquake Engineering*, Berkeley.
8. Dobry, R., Stokoe, K. H., Ladd, R. S. & Youd, T. L. (1981). Liquefaction susceptibility from s-wave velocity. *Proc. In situ Tests to Evaluate Liquefaction Susceptibility, ASCE National Convention*, St Louis, MO.
9. Dealba, P., Baldwin, K., Janoo, V., Roe, G. & Celikkol, B. (1984). Elastic-wave velocities and liquefaction potential. *Geotechnical Testing Journal*, Vol. 7, No. 2, 77-87.
10. Tokimatsu, K., Uchida, A. (1990). Correlation between liquefaction resistance and shear wave velocity. *Journal of Soils and Foundation*, Vol. 30, No. 2, pp. 33-42.
11. Rouch, A. F., Duffy, M., Stokoe, K. (2000). Laboratory correlation of liquefaction resistance with shear wave velocity. *Journal of Geotechnical and Geoenviromental Engineering, Geotechnical Special Publication*, Vol. 101, pp. 66-80
12. Huang, Y. T., Huang, A. B., Chen, K. Y. & Dou, T. M. (2004). A laboratory study on the undrained strength of a siltysand from central western Taiwan. *Journal of Soil Dynamic and Earthquake Engineering*, Vol. 24, No. 9-10, pp. 733-743.
13. Chen, Y.M., Ke, H. & Chen, R.P. (2005). Correlation of shear wave velocity with liquefaction resistance based on laboratory tests. *Journal of Soil Dynamics and Earthquake Engineering*, Vol. 25, 6, pp. 461-469.
14. Zhou, Y. G. & Chen, Y. M. (2005). Influence of seismic cyclic loading history on small strain shear modulus of saturated sands. *Journal of Soil Dynamic and Earthquake Eangineering*. Vol. 25, No. 5, pp. 341-353.
15. Ning Liu, S. M., Mitchell, J. K. & Hon, M. (2006). Influence of non plastic fines on shear wave velocity-based assessment of liquefaction. *Journal of Geotechnical and Geoenviromental Engineering*, Vol. 132, No. 8, pp. 1091-1097.

16. Zhou, Y. G. & Chen, Y. M. (2007). Laboratory investigation on assessing liquefaction resistance of sandy soils by shear wave velocity. *Journal of Geotechnical and Geoenviromental Engineering*, Vol. 133, No. 8, pp. 959-927.
17. Baxter, C. D. P., Bradshaw, A. S., Green, R. A. & Wang, J. (2008). Correlation Between Cyclic Resistance and Shear Wave Velocity for providence silts. *Journal of Geotechnical and Geoenviromental Engineering*, Vol. 134, No. 1, pp. 37-46.
18. Kayen, R., Seed, R. B., Moss R. E., Cetin K. O., Tanaka, Y. & Tokimatsu, K. (2004). Global shear wave velocity database for probabilistic assessment of the initiation of seismic-soil liquefaction. *11th Int. Conference on Soil Dynamics and Earthquake Engineering*, Berkeley.
19. Ladd, R. S. (1978). *Preparing test specimens using under compaction*. Printed by American Society for Testing and Material, pp.16-23.
20. Emery, J. J., Finn, W. D. L. & Lee, K. W. (1973). Uniformity of saturated sand samples. *ASTM Special Publishing*, pp. 182-194.
21. Ishihara, K. (1996). *Soil behavior in earthquake geotechnics*. Oxford Univ. Press, Newyork.
22. Koester, J. P. (1993). Effects of fines type and content on liquefaction potential of low-to medium plasticity fine-grained soils. *National Earthquake Conference*; *Earthquake Hazard Reduction in the Central and Eastern United States: Atime for Examination and Action*, pp. 67-75.
23. Seed, H. B., Idriss, I. M. & Arango, I. (1983). Evaluation of liquefaction potential using field performance data, *Journal of Geotechnical Engineering*, Vol. 109, No. 3, pp. 458-482.
24. Robertson, P. K. & Campanella, R G. (1985). Liquefaction potential of sands using CPT. *Journal of Geotechnical Engineering*, Vol. 111, No. 3, pp. 384-403.
25. Kuerbis, R., Negussey, D. & Vaid, V. P. (1988). Effect of gradation and fines content on the undrained response of sand. *Proceedings. Hydraulic Fill Structures*, Fort Collins, USA, pp. 330-345.
26. Pitman, T. D., Robertson, P. K. & Sego, D. C. (1994). Influence of fines on the collapse of loose sands. *Canadian Geotechnical Journal*, Vol. 31, No. 5, pp. 728-739.
27. Amini, F. & Qi, G. Z. (2000). Liquefaction testing of stratified silty sands. *Journal of Geotechnical and Geoenviromental Engineering, ASCE*, pp.208-217.
28. Tronsco, J. H. & Verdugo, R. (1985). Silt content and dynamic behavior of tailing sands. *Proc. Twelfth Int. Conference on Soil Mechanic and Foundation Engineering*, San Francisco, U.S.A, pp. 1311-1314.
29. Sladen, J. A., D'Hollander, R. D. & Krahn, J. (1985). Back analysis of the Nerk berm liquefaction slides. *Canadian Geotechnical Journal*, Vol. 22, No. 4, pp. 579-588.
30. Zelatovic, J. H. & Ishihara, K. (1985). Normalized behavior of very loose nonplastic soil: Effects of fabric. *Soils and Foundations*, Vol. 37, No. 4, pp. 47-56.
31. Lade, P. V. & Yamamuro, J. A. (1997). Effects of nonplastic fines on static liquefaction of sands. *Canadian Geotechnical Journal*, Vol. 34, No. 6, pp. 918-928.
32. Law, K. T. & Ling, Y. H. (1992). Liquefaction of granular soils with non-cohesive and cohesive fines. *Proceedings of the Tenth World Conference on Earthquake Engineering*, Rotterdam, pp. 1491-1496.
33. Singh, S. (1996). Liquefaction of silts and silty sands. *11th World Conference on Earthquake Engineering*, Elsevier.
34. Polito, C. P. & Martin, J. R. (2001). Effects of non plastic fines on the liquefaction resistance of sands. *Journal of Geotechnical and Geoenviromental Engineering*, Vol. 127, No. 5, pp. 408-415.
35. Xenaki, V. C. & Athanasopoulos, G. A. (2003). Liquefaction resistance of sand-silt mixtures: an experimental investigation of the effect of fines. *Journal of Soil Dynamic and Earthquake Engineering*, Vol. 23, No. 3, pp. 183-194.
36. Salgado, R., Bandini, P. & Karim, A. (2000). Shear strength and stiffness of silty sand. *Journal of Geotechnical and Geoenvironmental Engineering*, Vol. 126, No. 5, pp. 451-462.

37. Iwasaki, T. & Tatsuoka, F. (1977). Effects of grain size and grading on dynamic shear moduli of sands. *Soils and Foundations*, Vol. 17, No. 3, pp. 9-35.
38. Seed, H. B. & Peacock, W. H. (1971). The procedure for measuring soil liquefaction characteristics. *Journal of the Soil Mechanics and Foundation Division*, Vol. 97, SM8, pp. 1099-1119.
39. Finn, W. D. L., Pickering, D. J. & Bransby, P. L. (1971). Sand liquefaction in triaxial and simple shear tests. *Journal of the Soil Mechanics and Foundation Division*, Vol. 97, SM4, pp. 639-659.
40. Castro, G. (1976). Liquefaction and cyclic mobility of saturated sands. *Journal of Geotechnical Engineering Division*, Vol. 101, GT6, pp. 551-569.
41. Das, B. M. (1992). *Principles of soil dynamics*. Printed by: Pws-Kent Publishing Company.
42. Belloti, R., Jamiolkowski, J., LoPresti, D.C.F. & O'Niell, D. A. (1996). Anisotropy of small strain stiffness in Ticino sand. *Geotechnique*, Vol. 46, No. 1, pp. 115-131.
43. Tokimatsu, K., Yamazuka, T. & Yoshimi, Y. (1986). Soil liquefaction evaluations by elastic shear moduli. *Soils and Foundation*, Vol. 26, No. 1, pp. 25-35.
44. Lashkari, A. (2009). A constitutive model for sand liquefaction under rotational shear. *Iranian Journal of Science and Technology, Transaction B: Engineering*, Vol. 33, No. B1, pp.31-48.
45. Yegian, M. & Whitman, R. V. (1978). Risk Analysis for ground failure by liquefaction. *Journal of Geotechnical engineering division, ASCE*, Vol. 104, No. GT7, 921-938.
46. Haldar, A. & Tang, W. H. (1979). Probabilistic evaluation of liquefaction potential. *Journal of Geotechnical Engineering Division, ASCE*, Vol. 105, No. GT2, pp. 145-163.
47. Liao, S. C. C., Veneziano, D. & Whitman, R. V. (1988). Regression models for evaluating liquefaction probability. *Journal of Geotechnical Engineering Division*, Vol. 114, No. 4, Vol. 389-411.
48. Youd, T. L. & Noble, S. K. (1997). Liquefaction criteria based on statistical and probabilistic analyses. *Proc. NCEER Workshop on evaluation of liquefaction resistance of soils, Tech. Rep. NCEER-1997-0022, T. L. Youd and I. M. Idriss, eds., Nat. Ctr. for Earthquake Engineering Res*., State University of New York at Buffalo, Buffalo, pp. 201-215.
49. Toprak, S., Holzer, T. L., Bennett, M. J. & Tinsley, J. C. (1999). CPT- and SPT-based probabilistic assessment of liquefaction. *Proc. 7th U.S.-Japan workshop on earthquake resistance des. of lifeline fac. and Counter-measures against liquefaction, Multidisciplinary Center for Earthquake Engineering Research*, Buffalo.
50. Juang, C. H., Jiang, T. & Andrus, R.D. (2002). Assessing probability-based methods for liquefaction potential evaluations. *Journal of Geotechnical and Geoenvironmental Engineering, ASCE*, Vol. 128, No. 7, pp. 121-127.
51. Andrus, R. D., Piratheepan, P., Ellis, B. S., Zhang, J. & Juang, H. C. (2004). Comparing liquefaction evaluation methods using penetration Vs relationship. *Journal of Soil Dynamics and Earthquake Engineering*, Vol. 24, pp. 713-721.
52. Juang, H., Yang, S. H. & Yuan, H. (2005). Model uncertainty of shear wave velocity-based method for liquefaction potential evaluation, *Journal of Geotechnical and Geoenviromental Engineering, ASCE*, 1274-1282.
53. Cetin, K. O., Derkiurghian, A. & Seed, R. B. (2002). Probabilistic models for the initiation of seismic soil liquefaction. *Journal of Structural Safety*, Vol. 24, pp. 67-82.
54. Juang, C. H., Chen, C. J. & Jiang, T. (2001). Probabilistic framework for liquefaction potential by shear wave velocity. *Journal of Geotechnical and Geoenvironmental Engineering, ASCE*, pp. 670-678.
55. Duncan, J. M. & Hon, M. (1999). Factor safety and reliability in geotechnical engineering. *Journal of geotechnical and geoenvironmental engineering, ASCE*, pp. 1-38.
56. Dai, S. H. & Wang, M. O. (1992). Reliability analysis in engineering applications. Van Nostrand Reinhold, New York, pp. 433.